From Photon to Neuron

Princeton University Press, 2017

Supplementary Chapter

Philip Nelson

December 23, 2018

This chapter belongs to Part III (Advanced Topics). It is made freely available as-is in the hope that it will be useful. All reports of errata will be gratefully received: pcn@upenn.edu.

CHAPTER 17

Rainbows and Other Caustics

> Don't expect that mathematics will give you an easy answer to any physical problem. If you find that it does, that is evidence that you picked a poor problem to begin with.
>
> — *Blair Kinsman*

17.1 SIGNPOST: *BIFURCATIONS* OF STATIONARY-PHASE POINTS

If any physical phenomena can be called "beautiful," surely the rainbow is an example. Throughout human history it has played a key role in art, literature, and even religious scriptures, inspiring awe.[1] And yet, for millennia the rainbow was also a goad, a rebuke to humans' attempts to understand Nature. Practically every natural philosopher of any note had something to say about rainbows, yet very little was understood until René Descartes published an essay titled *La Dioptrique* in 1637.[2] We now see the rainbow as an exemplar of a much broader class of optical phenomena called "caustics." Phrased in modern language, we will see that Descartes correctly identified the origin of a caustic as a consequence of an even more broadly applicable concept called *bifurcation*: in this case, the merger and mutual annihilation of two stationary-phase points as a parameter is varied.

Figure 17.1 shows some features of the rainbow that are directly observable with the unaided eye. The Focus Question is

Question: What are the minimal requirements for the focusing of light? Can it happen naturally, or only with special apparatus?

Physical idea: Focusing to a bright line of light, with a diffuse background, is generic.

17.2 PRELIMINARIES

17.2.1 Natural versus contrived focusing

Chapter 6 discussed the focusing of light by a lens. Focusing to a point turned out to be a tricky affair, requiring the lens to have the right shape and distance to a focusing screen. In constrast, another form of focusing arises naturally and is ubiquitous. For example, sunlight that arrives at the bottom of a swimming pool gets concentrated into a network of bright *lines* (not points). The constantly changing shape of the water surface (due to wind) does not destroy these lines, but merely moves them. A partial focus of this sort is generically called a **caustic**; point focus is just one special case.

In general, the projection of a caustic onto a viewing screen lies along a line. Because the screen need not be at any special distance from the source, the caustic itself occupies a 2D *surface* in 3D space.

---

[1] Awe and *fear:* Many folk traditions attribute grim consequences to pointing at a rainbow.

[2] Thomas Harriot performed similar calculations 30 years earlier, but apparently never published them.

Figure 17.1: [Photograph.] **Rainbow.** Note (*i*) the sky appears darker between the two bows; (*ii*) the secondary bow is less bright than the primary; (*iii*) the order of colors is opposite in the two bows; (*iv*) the main bow's color sequence is ROYGVGVG. The faint, extra last bands are part of a "supernumerary" bow; see Section 17.3.4. The photo was taken with a polarizing filter; this does not affect the rainbow, which is already polarized, but it does reduce background light from the sky. *Inset:* Color saturation was digitally enhanced to bring out the structure. [Photo courtesy Steve Nelson (Fayfoto, Boston MA).]

We will soon see that a natural rainbow involves a particular kind of caustic.

17.2.2 Dispersion from a triangular prism

Section 5.3.5 introduced the concept of dispersion: Because different vacuum wavelengths travel at slightly different speeds in a transparent medium, the bending predicted by the law of refraction is wavelength-dependent. Figure 17.2 shows the resulting behavior in a macroscopic setting. A bundle of parallel incoming rays of light[3] gets spread in angle upon entering a prism, then spread further upon exiting.

A key observation is that each spectral color exits at a specific angle relative to the incoming rays, and that this angle is the same for each of the parallel incoming rays. Thus, as we move farther away from the prism, the increasing spread with distance eventually dominates the smearing from finite beam width, and a clear spectrum emerges.

[3]Section 6.5.1 introduced the concept of light rays.

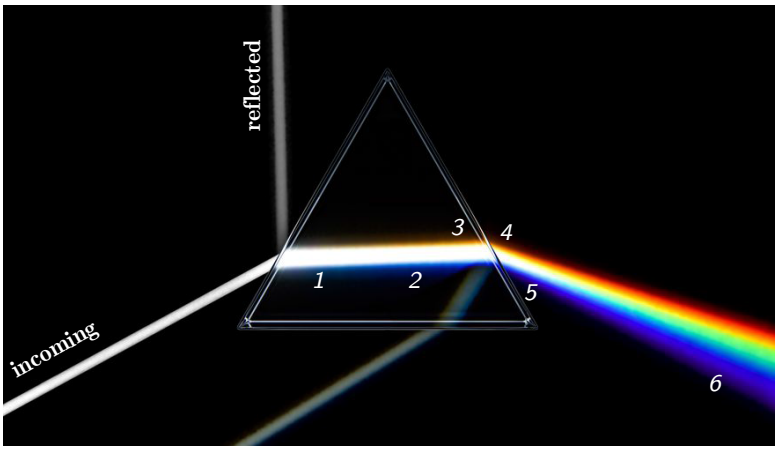

Figure 17.2: [Photograph.] **Colors from a prism.** *1*: Each incoming ray bends toward the perpendicular upon entry. *2,3*: Blue is bent slightly more than red. *4*: A bundle of many parallel incoming rays combine their respective spectra, leaving mostly white except at the edges. *5*: Each ray bends away from the perpendicular upon exit, and again blue bends more. *6*: Each color emerges at a specific angle, which is the same for each of the parallel incoming rays. [`https://sciencing.com/happens-light-passes-through-prism-8557530.html`]

17.3 SPHERICAL DROPLETS: THE CARTESIAN RAINBOW

17.3.1 The rainbow as a caustic

Rainbows are always seen with the Sun behind the observer. Eventually, early scientists realized that the light we see must be sunlight scattered backward to us from water droplets in the sky. Figure 17.3 shows how this is possible: Light rays are shown entering a droplet, then partially reflecting inside it. (Much of the incoming light instead exits the droplet at point **Q**, continuing away from the observer, but some will be internally reflected.) As with the prism, two rounds of refractive bending are involved, and each can spread incoming white light.

Closer inspection of Figure 17.3 reveals a problem with this explanation, however. For the case of a spherical water droplet in air, outgoing ray directions depend on wavelength, but also on *which ray* we are following, so that a jumble arrives on any projection screen. How, then, can we get a rainbow? Here is where Descartes made his decisive contribution.

Descartes realized that although an incoming bundle of parallel rays will emerge in many directions, nevertheless there is a *minimum angle* of deviation. That is, in the ray-optics approximation no light will be returned at angles less than this minimum. (Larger angles all the way up to 180 deg are all possible.) You should stop reading now and work out the details in Problem 17.1. A key conclusion is that a projection screen placed behind the droplet will catch light covering a disk-shaped region, leaving the exterior of that disk dark, and moreover *the edge of the disk will be especially bright.* In fact, the edge is a caustic.

Descartes confirmed the predicted phenomena with an experiment in which a spherical flask of water was illuminated by a shaft of sunlight in an otherwise dark room.

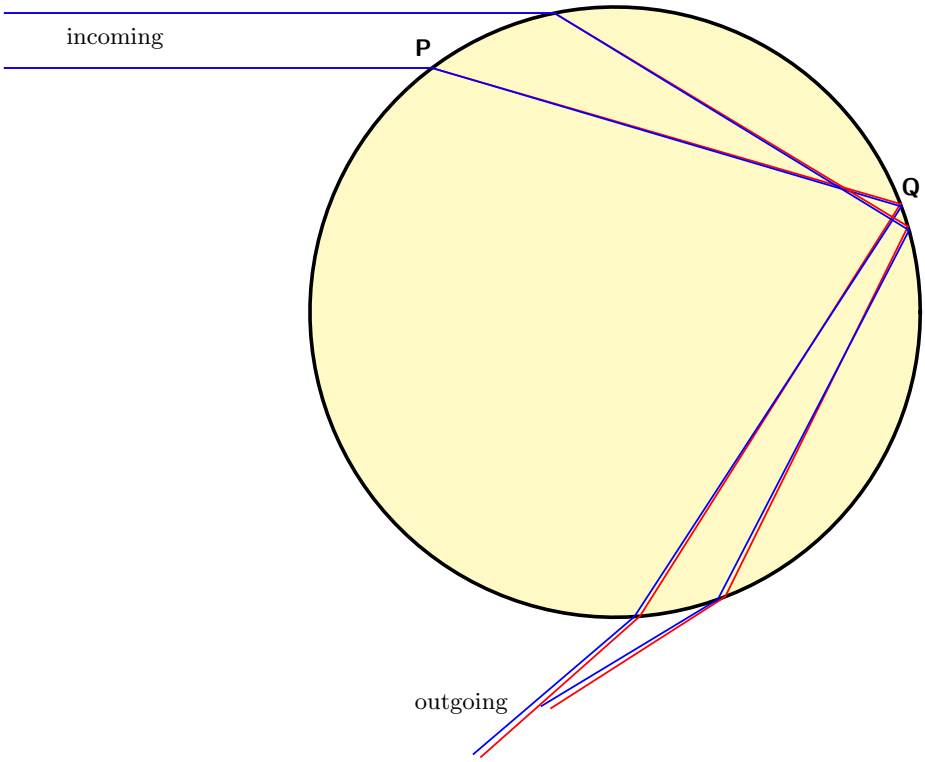

Figure 17.3: [Ray diagram.] **Parallel incoming rays emerge nonparallel from a droplet.** The red and blue lines depict rays that obey the laws of reflection and refraction for two different wavelengths. *Not shown:* Much of the incoming light exits at point **Q**, but we are interested in the part that internally reflects as shown. (Also, some of the incoming light reflects at **P**.)

17.3.2 The primary bow arises from one internal reflection

When we see a rainbow, we are looking not at a single object, but at the combined effects of countless droplets. Descartes drew a diagram similar to Figure 17.4 to explain the situation:

- Each droplet reflects light back in a caustic shaped like a cone, with the droplet at its apex. Even if the droplets are not all the same size, each of their cones has the same opening angle, because that angle does not depend on the size.
- We can catch part of that droplet's cone of light if our angle of view relative to the Sun's rays equals the cone's opening angle.
- The locus of all points in space that meet this condition is also a cone, but with our eye at the apex: When we look in a direction lying on that cone, we see glints from every droplet lying along that line of sight.

The combined effect is an apparent glowing arch in the sky.

Descartes did not have the framework needed to complete his understanding of the rainbow, because he did not understand that white light is a mixture of different spectral colors. Shortly after his work, Newton pointed out that each spectral component of light will have a slightly different angular radius for its bright ring, so that the ring will appear colored. The weaker light sent to larger scattering angles creates a

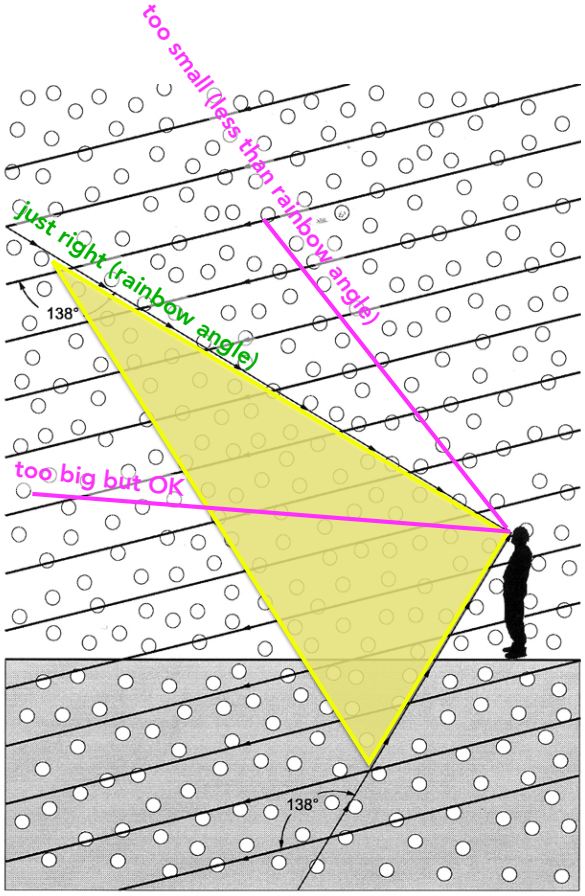

Figure 17.4: [Diagram.] **When many droplets are present, we only see light from a few.** Atmospheric scientist Craig Bohren observes reflected light mainly originating from droplets located on a cone with half-angle 0.7 rad, that is, from directions rotated 2.4 rad from that of the incoming solar rays. The upper part of this cone appears to the observer as a partial ring of light. The lower part is mostly preempted by the Earth; that it, it has very little optical depth, and so is not visible, unless the observer is in an airplane. [From Bohren & Clothiaux, 2006.]

diffuse, white illumination inside the bow. Indeed, real rainbows are noticeably darker just outside the ring than inside (Figure 17.1).

17.3.3 The secondary bow arises from double internal reflection

In good conditions a second bow is often visible (Figure 17.1). It has a similar explanation, involving *two* internal reflections. Because each reflection is only partial, the secondary bow is usually less bright than the primary. Because the total scattering angle is now greater than 180 deg, the extra bending of blue relative to red implies that the order of colors is reversed relative to the primary bow, as is also seen in Figure 17.1.

17.3.4 Critique of ray-optics results

Ray optics has given us a good account of several of the properties of rainbows. Conspicuously absent from the list, however, is any explanation of the "supernumerary" bows that are visible in Figure 17.1. It is easy to miss this phenomenon if you are not looking for it. Even if you look it is not always visible, and artistic depictions almost never include it. Perhaps for these reasons, as well as the overwhelming authority of

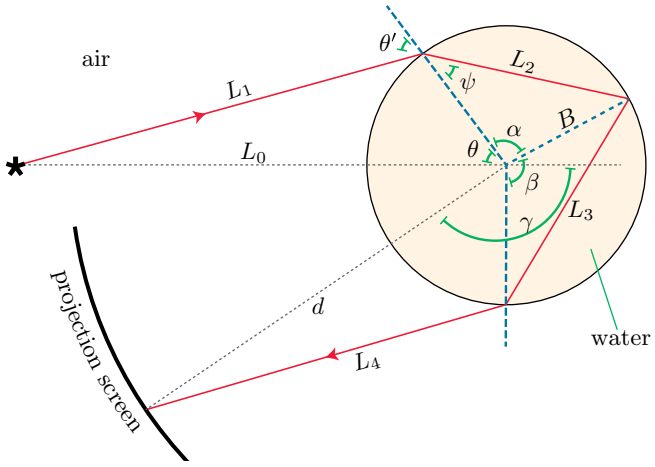

Figure 17.5: [Diagram.] **Scattering geometry.** Light from a distant point source scatters from a droplet through angle γ and lands on a distant projection screen. The path shown is not a stationary phase path. The diagram is not to scale; the main text considers only the case $L_0 \gg B$ and $d \gg B$. In that limiting case, the angles θ' and θ become equal.

Isaac Newton, the supernumerary bows were dismissed until Thomas Young offered them as evidence for the wavelike aspect of light in 1803.

Young pointed out that for scattering angle γ greater than the caustic value γ_* (that is, within the primary bow) there are *two* different incoming rays (two stationary-phase paths) of unequal length that emerge at that angle.[4] The path-length difference depends on γ, leading to an interference pattern of light and dark bands, different for each wavelength. Young proposed that these considerations could explain the supernumerary bows.

Although Young's idea was correct in essence, it is not a quantitative theory: It attempts to join together the ray-optics approach, which suppresses the wavelike character of light, with interference, which is inherently a wave phenomenon. Section 17.4 will outline a more self-consistent calculation.

Moreover, the calculation you did in Problem 17.1 appears to predict an *infinite* intensity of light right at the caustic! This unphysical prediction, too, is an pathology of the ray-optics approximation, as we will now see. It is similar to the conclusion from ray-optics that a lens can focus light down to a mathematical point. Really, we know that diffraction limits the focus of even a perfect lens;[5] similarly, we will find finite light intensity at the rainbow caustic.

17.4 THE DIFFRACTIVE RAINBOW

17.4.1 Stationary-phase paths can be created and lost as parameters are changed

Figure 17.5 assigns names to the quantities that appear below. As in earlier chapters, we restrict attention to paths that consist of straight lines within each medium, with sharp bends or bounces only at the boundaries between media. However, and also as in earlier chapters, we do not insist on the rules of ray optics (laws of reflection or refraction); these will emerge in the course of finding the stationary-phase path(s).

[4] You should have found this when solving Problem 17.1. More precisely, this holds for scattering γ angles greater than the caustic value, but less than about 2.8 rad.
[5] See Section 6.8.1.

According to the Light Hypothesis,[6] the path shown contributes a phase equal to $2\pi/\lambda$ times

$$L_{\text{eff}} = L_1 + nL_2 + nL_3 + L_4, \tag{17.1}$$

where n is the index of refraction of water at the wavelength of the light.

To simplify the calculations, we will illustrate the method in two dimensions, that is, neglect the third dimension coming out of the page. We'd like to compute the probability amplitude for photon arrivals at a particular point on the projection screen, that is, a particular value of the angle γ. This will be the sum of contributions for various paths, that is, for various values of the angles θ, α, and β that characterize each path.

We are interested in the situation where the source distance L_0 is much larger than the droplet radius B. As in Chapters 5 and 6, this means that the incoming part of the path has the simple form

$$L_1 = L_0 - B\cos\theta + \cdots,$$

where the ellipsis denotes terms that vanish as $B/L_0 \to \infty$. Similarly, because $d \gg B$ we have

$$L_4 = \sqrt{(d\cos\gamma - (-B\cos(\theta+\alpha+\beta)))^2 + (-d\sin\gamma - (B\sin(\theta+\alpha+\beta)))^2} \tag{17.2}$$

$$= d + B\cos(-\gamma+\theta+\alpha+\beta) + \cdots, \tag{17.3}$$

where again the ellipsis indicates terms we may drop.

The two isosceles triangles in Figure 17.5 have

$$L_2 = 2B\sin(\alpha/2) \text{ and } L_3 = 2B\sin(\beta/2).$$

Our previous experience suggests that, for millimeter-scale droplets, the most significant contributions to the answer will come from stationary-phase paths and their immediate neighbors. To find them, we now fix a point on the observation screen (that is, γ is a constant γ_0) and consider small variations about a particular path:

$$\theta = \theta_0 + \xi, \quad \alpha = \alpha_0 + \nu, \quad \beta = \beta_0 + \mu.$$

It will also be convenient to define $\Lambda = -\gamma_0 + \theta_0 + \alpha_0 + \beta_0$.

We now expand L_{eff} as a Taylor series in ξ, ν, and μ:

$$L_{\text{eff}} = L_{\text{eff}}^{(0)} + L_{\text{eff}}^{(1)} + L_{\text{eff}}^{(2)} + \cdots.$$

The first ("zeroth-order") term is an irrelevant constant. The first-order term is

$$L_{\text{eff}}^{(1)} = B[\xi(\sin\theta_0 - \sin\Lambda) + \nu(n\cos(\alpha_0/2) - \sin\Lambda) + \mu(n\cos(\beta_0/2) - \sin\Lambda)].$$

For a stationary-phase path, we require that all three of these terms be zero. Thus, $\sin\theta_0$, $n\cos(\alpha_0/2)$, and $n\cos(\beta_0/2)$ must all equal $\sin\Lambda$ (and hence must equal each other). We restate this as

$$\alpha_0 = \beta_0 \tag{17.4}$$

$$\sin\theta_0 = n\cos(\alpha_0/2) \tag{17.5}$$

$$\theta_0 = \text{either } \Lambda \text{ or } (\pi - \Lambda). \tag{17.6}$$

[6] Ideas 4.5 and 4.6.

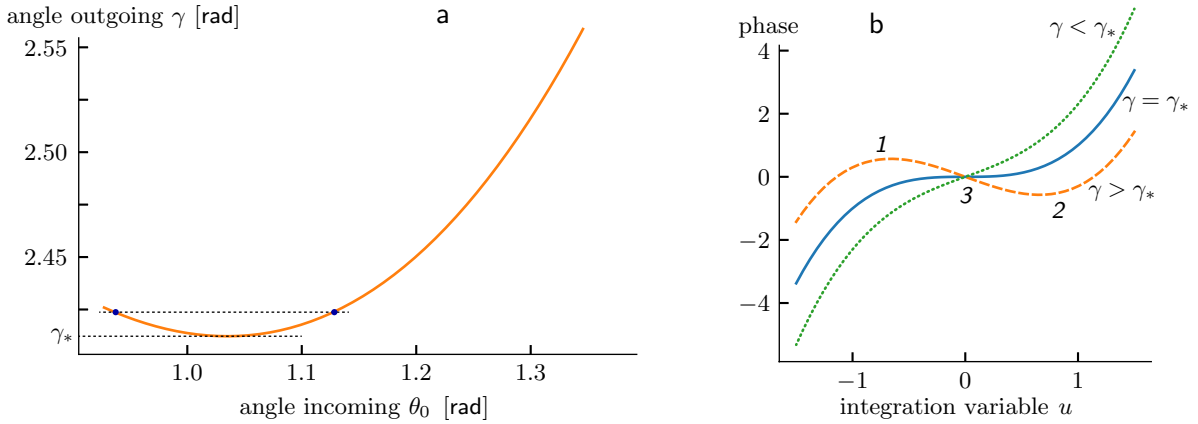

Figure 17.6: [Mathematical functions.] **Behavior near a caustic.** (a) Stationary-phase paths can be labeled by the angle θ_0 of their entry point, or by their exit angle γ. For some values of γ there are two such paths (*dots*); for others there are none ($\gamma < \gamma_*$). (b) A simplified situation with only one integration variable u, showing how two stationary-phase points (*1* and *2*, *orange dashed curve*) can merge (*3*, *blue solid curve*) and then disappear (*green dotted curve*) as a control parameter is adjusted through a special value.

The first of these conditions is just the law of reflection. Figure 17.5 shows that the angle of refraction is $\psi_0 = (\pi - \alpha_0)/2$, so Equation 17.5 is the law of refraction at the entry point. The last condition has two cases because $\sin(\pi - x) = \sin x$, but the first is spurious; we are interested in the second, which is the law of refraction at the exit point.

Thus, we have recovered the rules of ray optics. You already know the solution from Problem 17.1: Equations 17.4–17.6 have *two* solutions for large angles γ, and *no* solutions for smaller γ. That is, as we move on the projection screen from larger to smaller scattering angles (away from the "antisolar point"), the two stationary-phase points approach each other, merge, and *disappear*. We say that the phase suffers a **bifurcation** from two to zero stationary-phase points.[7]

17.4.2 The caustic angle arises as a bifurcation point

We are particularly interested in the special value γ_* at which the two stationary-phase paths merge. This is the caustic, and it is where ray optics approximation broke down (it gave us the unphysical result of infinite probability density). To find it, combine Equations 17.4–17.6 to get

$$\gamma = 2\theta_0 + 4\cos^{-1}(n^{-1}\sin\theta_0) - \pi. \tag{17.7}$$

Figure 17.6a shows this function. It is minimum when

$$\tfrac{1}{2}n\sin(\alpha_*/2) = \cos\theta_*. \tag{17.8}$$

Use Equation 17.5 to eliminate α_*:

$$2n^{-1}\cos\theta_* = \sqrt{1 - n^{-2}\sin^2\theta_*}$$

[7] "Catastrophe theory" studies a wide range of phenomena involving bifurcations of the stationary points of a function. For example, each curve of Figure 17.6b could represent the potential energy of a system; as the control parameter changes, the stable minimum disappears altogether, with consequences that could indeed be catastrophic in the nonmathematical sense of the word.

$$\sin\theta_* = \sqrt{(4-n^2)/3}. \tag{17.9}$$

For water in air, evaluating this expression and substituting in Equation 17.7 gives the caustic's angle (in this situation called the **rainbow angle**) as $\gamma_* \approx 2.41$, as seen in the figure.

17.4.3 The Light Hypothesis addresses the shortcomings of ray optics

Figure 17.6b shows a simplified version for the mathematical behavior we have found: The horizontal axis shows a single variable u schematically representing all three integration variables ξ, μ, and ν. The three curves show imagined behavior above, at, and below a critical value of the control parameter γ. We see two stationary points that move together, merge, and disappear. Such mergers are examples of bifurcations.

What happens to the probability amplitude for photon arrivals when this merger occurs? The situation is reminiscent of the one discussed in Chapter 6. With no lens, many points on the projection screen each have a phase function with a single stationary-phase point u_*. With a lens, however, one point in space is special. The special point lies in the plane at distance d satisfying the focus condition. Within that plane, it is located along the straight line from the source that passes through the lens center, that is, at $x = 0$ in Figure 6.3. This point has a phase function whose graph is flatter than an ordinary stationary-phase point: It is a constant plus a u^4 term (not u^2).[8] The sum of contributions to the probability amplitude then has a longer central region than the one shown in Figure 4.11a, and hence its modulus squared is large, leading to very bright illumination at that one spot.

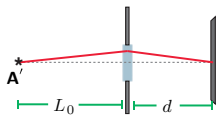

Fig. 6.3

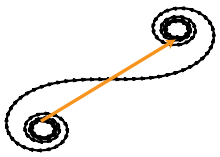
Fig. 4.11a

Similarly, above the caustic angle the dashed curve in Figure 17.6b has two stationary-phase points (marked *1* and *2* on the dashed curve), each leading to a large excursion in the complex plane in between tight coils. Those excursions can either reinforce (Figure 17.7a) or cancel (Figure 17.7b), depending on the length difference of the two corresponding paths. The resulting interference pattern is wavelength-dependent, potentially explaining the colored supernumerary bows.

Just at the caustic angle, there is only a single stationary-phase point (solid curve in Figure 17.6b), but the phase function is flatter there than in the generic case: As a function of u, the leading behavior is u^3, not u^2. Accordingly, the resultant is especially big there (Figure 17.7c), giving rise to the bright caustic ring. However, in contrast to the ray-optics theory, the light intensity is *finite* at the caustic.

For scattering angles less than the caustic angle, there is no stationary-phase point at all (dotted curve in Figure 17.6b), analogously to a defocused lens system. The integral that yields the probability amplitude consists mostly of tight spirals, so its modulus squared is small (Figure 17.7b). Unlike in ray optics, however, there is *some* illumination inside the caustic angle.

Figure 17.8 summarizes the qualitative expectations raised in this section.

17.4.4 Confirm expectations

To justify our expectations, we must now look at the higher-order terms in L_{eff} (Equation 17.1). Up till now, we have only expanded this function to first order in small variations around chosen starting values of θ_0, α_0, and β_0.

To begin, we will examine the phase function for an observer located at the caustic angle, that is, set γ equal to the value γ_* found below Equation 17.9. The sketch graph

[8] See Figure 6.4.

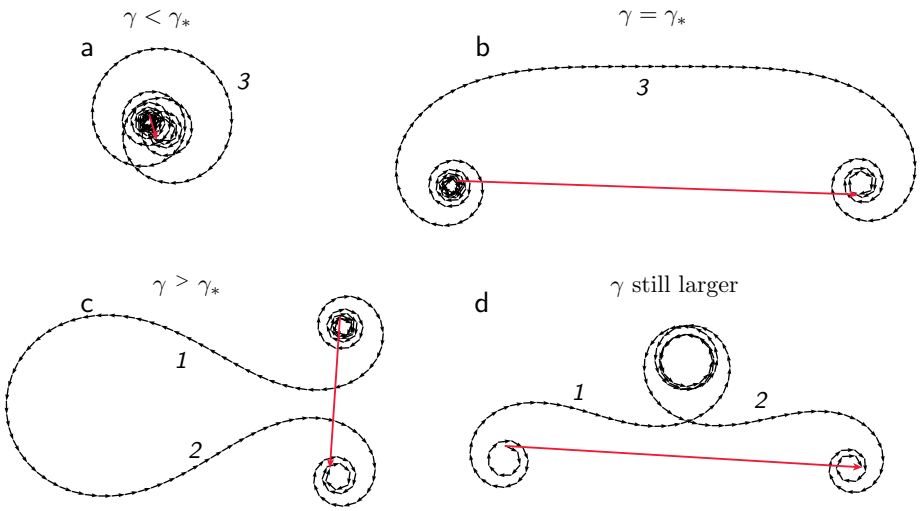

Figure 17.7: [Sketch graphs.] **Contributions to the probability amplitude,** corresponding to the three cases shown in Figure 17.6b. Each panel represents an integral in the same style as Figure 4.11. In each case, the *red vector* is the resultant from adding many contributions (*black arrows*). *Number labels* refer to features in Figure 17.6b. (a) At scattering angles below γ_*, there is no stationary-phase path at all. (b) Exactly at the caustic angle, we get super-constructive interference. (c,d) Beyond the caustic angle, the two stationary-phase paths each make contributions similar to Figure 4.11a. These can interfere constructively or destructively.

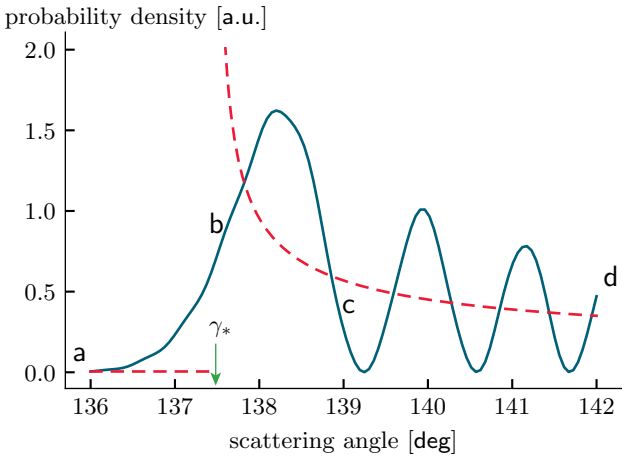

Figure 17.8: [Mathematical functions.] **Models of the rainbow.** *Dashed curve:* Ray optics predicts zero light below the caustic angle and infinite intensity right at it (see Problem 17.1). *Solid curve:* The sum over paths correctly predicts: (a) Some light below the caustic angle; (b) finite intensity at every scattering angle; and (c–d) an interference pattern above the caustic angle. The calculation assumed an index of refraction 1.33 and droplet radius B related to light wavelength by $B = 1500\lambda/(2\pi)$, and neglected the contribution from paths that reflects off the droplet surface instead of entering it. (If included, such contributions would superimpose rapid variations on the same overall structure shown here.)

(solid curve in Figure 17.6b) suggests that we are looking for a flat region of the phase function, but there are *three* integration variables—not just one as in the figure. At least we know where to look: The stationary-phase path is at $\theta_0 = \theta_*$, $\alpha_0 = \alpha_*$, and $\beta_0 = \alpha_*$ given by Equations 17.8 and 17.9.

As previously, we now let ξ, ν, and μ be small deviations of θ, α, and β away from the starting point. We already know that the phase function's variation vanishes at first order in these deviations, so we now collect the second-order terms:

$$L_{\text{eff}}^{(2)} = \tfrac{1}{2}B\big[\xi^2\cos\theta_* + (\nu^2+\mu^2)\frac{-n}{2}\sin(\alpha_*/2) - (\xi+\nu+\mu)^2\cos\Lambda_*\big].$$

In the second term, note that $\sin(\alpha_*/2) = \sqrt{1 - n^{-2}\sin^2\theta_*}$. In the last term, note that $\cos\Lambda_* = -\cos\theta_*$. Thus,

$$L_{\text{eff}}^{(2)} = \tfrac{1}{2}B\Big[(2\xi^2 + \nu^2 + \mu^2 + 2\xi\nu + 2\xi\mu + 2\nu\mu)\cos\theta_* - (\nu^2 + \mu^2)\frac{n}{2}\sqrt{1 - n^{-2}\sin^2\theta_*}\Big].$$

Next, note that Equation 17.9 says $\cos\theta_* = \sqrt{(n^2-1)/3}$ and $\frac{n}{2}\sqrt{1 - n^{-2}\sin^2\theta_*} = \sqrt{(n^2-1)/3}$. Thus,

$$L_{\text{eff}}^{(2)} = \tfrac{1}{2}B\sqrt{(n^2-1)3}\begin{bmatrix}\xi & \nu & \mu\end{bmatrix}\begin{bmatrix}2 & 1 & 1\\ 1 & 0 & 1\\ 1 & 1 & 0\end{bmatrix}\begin{bmatrix}\xi\\ \nu\\ \mu\end{bmatrix}.$$

Although the quadratic terms do not cancel completely, we see that *at the caustic, one direction is singular.* That is, the matrix just found has one zero eigenvector, namely the one with $\nu = \mu = -\xi$. This one direction in the path integral becomes degenerate as we sweep γ through the caustic, leading to the behavior anticipated in Section 17.4.3.[9] In particular, the phase near $\nu = \mu = \xi = 0$ is super-stationary in the special direction, leading to a large, but finite, enhancement in intensity at the caustic.

For values of γ close, but not equal, to γ_*, the phase acquires linear terms even when traversed along the special direction just found. In this way, we see that the picture in Figure 17.6 captures the essential physics. Nothing significant changes in the other two integration directions near the caustic, so we may replace those integrations by constants.

17.4.5 Reduction to a single integral

For the simplest possible calculation, we just replace the full three-dimensional integral over θ, α, and β by a single integral along the line that passes through $(\theta_*, \alpha_*, \beta_*)$ and is directed along the degenerating direction just identified. Because nothing is degenerating in the other two directions of the path integral, we may hope that the remaining two integrals in directions transverse to the interesting one roughly contribute a constant factor.[10] Figure 17.8 shows the result of evaluating the remaining integral numerically, then computing its modulus squared. Labeled points correspond to the examples shown in Figure 17.7, illustrating:

(a) Small (but nonzero) probability in the zone that was forbidden in ray optics approximation.
(b) Finite probability at γ_*.
(c) Nonmonotonic falloff (supernumerary bows) beyond the caustic.

G. Airy carried out an analysis roughly equivalent to the preceding discussion in 1838, though from a different viewpoint. He concluded as we did that diffractive scattering near the caustic was dominated by an oscillatory integral whose phase is a degenerating family of cubic functions. The answer as a function of the control parameter γ is now called the **Airy function**; its modulus squared gives rise to the solid curve in Figure 17.8.

[9] This result is similar to the analysis of Problem 6.8.
[10] We use a similar argument to avoid nonplanar paths, that is, to avoid having to do a *six*-dimensional integral over the entry, exit, and reflection points.

17.5 VISTA

17.5.1 Contrast to point focus

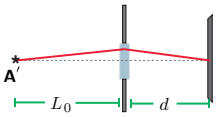

Fig. 6.3

Recall the situation with point focusing. For simplicity, consider the two-dimensional case (Figure 6.3). Focusing to a point required two conditions: (*i*) The distance d to the projection screen had to have the correct value given the distance L_0 the lens focal length. (*ii*) The observer had to sit at the correct point on the projection screen. When these two conditions were met, then we found a value u_* of u at which the phase function $\varphi(u)$ acquired three special properties: Its Taylor series expansion about u_* was a constant plus terms of order at least $(\delta u)^4$; that is, the linear, quadratic, and cubic terms were missing, leading to a big enhancement of probability amplitude.[11] In short,

(two conditions) + (freedom to choose u_*) $\rightarrow$ three special properties of $\varphi(u)$ about u_*.

Now think about what we found for the caustic, again in two dimensions. Here we only had to impose one condition: The screen could be at any (large) distance and the sphere could have any radius, so the only condition is that the scattering angle have a particular value γ_*. We had three integration variables, so the freedom to choose their three starting values was sufficient to eliminate their three linear coefficients in the phase function. The condition on scattering angle then sufficed to gain *one* additional property, that in one integration direction the quadratic part of the phase function should also vanish. This was enough to make the phase function super-stationary, though not as much as in the point focus. In short,

(one condition) + (freedom to choose θ_*, α_*, β_*) $\rightarrow$ four special properties of $\varphi(u)$.

In three dimensions, a similar counting argument predicts that generically a curved transparent object can focus light to a *surface* in space, that is, the locus where again one condition is satisfied—a caustic.

17.5.2 Droplet size and shape effects

Earlier we saw that the value of the caustic angle γ_* does not depend on droplet size B. Certainly the dispersion (wavelength dependence of the index of refraction) does not depend on B either, so droplets of every size give the same rainbow caustic: The variation of droplet sizes found in real atmospheric systems does not destroy the rainbow.

Matters are more complicated when we turn to interference effects, because now there is a new length scale—the physical wavelength of light matters. Similarly to the case of finite slit diffraction, droplet size now affects the interference, and a mixture of droplet sizes will blur out the supernumerary bows.

However, smaller droplets are more nearly spherical than larger ones, because for them surface tension dominates over air drag forces. When we look at the upper part of a rainbow, the dependence of arc position on droplet size mentioned in the preceding paragraph can be partially canceled by an *opposite* dependence from the slightly ellipsoidal cross-section of the larger droplets; when this occurs, the supernumeraries can be distinguished (Figure 17.1).

[11] Actually, we added a third condition, that the lens shape had to be symmetrical about $u = 0$. But the only role of this condition was to ensure that $u_* = 0$, simplifying the problem.

When we look at the lower part of the rainbow, the scattering occurs in a mostly horizontal plane. In this plane, each droplet's cross-section is circular, so the cancellation mechanism just described cannot occur. Indeed, supernumerary arcs are generally not seen in the lower part of a rainbow (Figure 17.1).

17.5.3 Polarization and other effects

The discussion in this chapter is far from being the last word on rainbows. Airy's work preceded, and so could not incorporate, Maxwell's theory of the connection between light, electricity, and magnetism. For example, our presentation so far has neglected the transverse character of light, and in particular the polarization dependence of the transmission and reflection coefficients.[12] In fact, however, for the dominant polarization of scattered light our calculation agrees quite closely with a sophisticated model based on Maxwell's equations. (For the other polarization, nearly all light exits the sphere instead of reflecting internally.)

THE BIG PICTURE

The rainbow reminds us that concepts from one domain of experience can be unexpectedly relevant in an apparently distant context: For example, the idea of *bifurcation* from dynamical systems proved to be key to unraveling the structure of caustics.

Even at the level of raw phenomena, we may find something salient (for example, a beautiful rainbow), think about it, and extract a more general class of phenomena (caustic focusing) that we had not previously thought to explore systematically. For example, the twinkling of stars in the night sky results when caustic surfaces, caused by nonuniformity in atmospheric temperature, sweep across our eyes. In a biophysical setting, caustics are important for the visual ecology of shallow-water marine creatures, which must deal with photodamage from greater fluctuations of light intensity than we might have expected; they must also make sense of their visual world amid large distracting dynamic illumination patterns; and so on. Surely we have not yet learned the last lessons that rainbow can teach us.

FURTHER READING

Semipopular:
Lynch & Livingston, 2001; Lee, Jr. & Fraser, 2001; Boyer, 1987.

Intermediate:
Bohren & Clothiaux, 2006, §8.4.2; Nye, 1999.
Descartes experiment: Ivanov & Nikolov, 2016.

Technical:
Berry, 2015; Nussenzveig, 1992.

[12] In addition, these coefficients are not independent of angle as we assumed; Idea 5.1 only gave them for the case of perpendicular incidence.

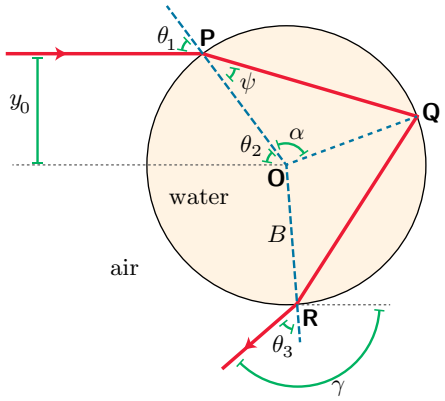

Figure 17.9: [Ray diagram.] **See Problem 17.1.**

PROBLEMS

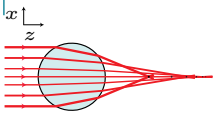

Fig. 6.10a

17.1 *Ray-optics rainbow*

In this problem, you'll make a picture like Figure 6.10a, but instead of following the transmitted ray you'll examine the internally reflected ray, and use index of refraction values appropriate for a spherical water droplet in air. Use the ray-optics approximation for this problem, and restrict everything to a plane passing through the droplet center.

a. Consider a set of parallel incoming rays, traveling horizontally in Figure 6.19. One incoming ray arrives at distance y_0 from the centerline, as shown. Find the angle θ_2 shown in terms of y_0 and the sphere radius B. Explain why the ray's angle of incidence θ_1 equals θ_2.

b. Use the law of refraction to find the angle ψ in terms of θ.

c. The triangle **PQO** is isosceles. Use that fact to find the angle α in terms of θ_2.

d. Use the law of reflection to conclude that the triangles **PQO** and **QRO** are congruent, and hence to find the point of exit, **R**.

e. Use the law of refraction again to show that $\theta_3 = \theta_1$. Then find the angle γ that the exiting ray makes with the right-pointing horizontal after exiting the droplet. This angle will lie between $\pi/2$ and π, because the exiting ray is scattered backward.

f. Use a computer to draw the four segments of this ray, and repeat for a range of other y_0 values. (Also draw the circular boundary of the droplet's cross-section as shown.)

g. Make a graph showing the angle γ as a function of y_0.

h. Suppose that incoming light is uniformly distributed across the water drop, that is, y_0 is a Uniform random variable. Conclude that the exit angle you found in (g) is nonuniformly distributed, and describe its PDF qualitatively.

i. If the incoming light is monochromatic, what would you expect to see projected onto a screen that intercepts these rays? What if the incoming light is white?

17.2 *Diffractive rainbow*

[Not ready yet.]